JBC RESEARCH ARTICLE

ADAR promotes USP38 auto-deubiquitylation and stabilization in an RNA editing–independent manner in esophageal squamous cell carcinoma

Received for publication, April 10, 2024, and in revised form, August 31, 2024 Published, Papers in Press, September 19, 2024,
https://doi.org/10.1016/j.jbc.2024.107789

Qingyong Hu[1,‡,*], Yahui Chen[1,‡], Qianru Zhou[1], Shanshan Deng[1], Wei Hou[1,2], Yong Yi[3], Chenghua Li[3], and Jiancai Tang[1,*]

From the [1]Institute of Basic Medicine and Forensic Medicine, North Sichuan Medical College, Nanchong, Sichuan, China; [2]Department of Pathology, Affiliated Hospital of North Sichuan Medical College, Nanchong, China; [3]Center of Growth, Metabolism and Aging, Key Laboratory of Biological Resources and Ecological Environment of Ministry of Education, College of Life Sciences, Sichuan University, Chengdu, China

Reviewed by members of the JBC Editorial Board. Edited by Donita C. Brady

Esophageal cancer is mainly divided into esophageal adenocarcinoma and esophageal squamous cell carcinoma (ESCC). China is one of the high-incidence areas of esophageal cancer, of which about 90% are ESCC. The deubiquitinase USP38 has been reported to play significant roles in several biological processes, including inflammatory responses, antiviral infection, cell proliferation, migration, invasion, DNA damage repair, and chemotherapy resistance. However, the role and mechanisms of USP38 in ESCC development remain still unclear. Furthermore, although many substrates of USP38 have been identified, few upstream regulatory factors of USP38 have been identified. In this study, we found that USP38 was significantly upregulated in esophageal cancer tissues. Knockdown of USP38 inhibited ESCC growth. USP38 stabilized itself through auto-deubiquitylation. In addition, we demonstrate that adenosine deaminase acting on RNA (ADAR) could enhance the stability of USP38 protein and facilitate USP38 auto-deubiquitylation by interacting with USP38 in an RNA editing–independent manner. ADAR inhibition of ESCC cell proliferation depended on USP38. In summary, these results highlight that the potential of targeting the ADAR–USP38 axis for ESCC treatment.

Cancer is one of the most challenging health issues globally, posing a serious threat to human health and social development. Research evaluations indicate that China had approximately 4.82 million new cancer cases and 2.57 million cancer deaths in 2022 (1). Lung cancer, liver cancer, gastric cancer, colorectal cancer, and esophageal cancer are the top five causes of cancer death in China, accounting for 67.50% of total cancer deaths (1). Esophageal cancer is mainly divided into esophageal adenocarcinoma and esophageal squamous cell carcinoma (ESCC) (2). China is one of the high-incidence areas of esophageal cancer, of which about 90% are ESCC (3). However, its heterogeneity and complexity still require in-depth research. The early symptoms of esophageal cancer are not obvious, and patients are often diagnosed at late stages, resulting in poor treatment outcomes. Therefore, early diagnosis and prevention of esophageal cancer remains a huge challenge. The main treatments for esophageal cancer patients include surgery, radiotherapy, and chemotherapy (4, 5). However, surgery may not be suitable for some esophageal cancer patients due to the location of the lesion or the advanced stage of the disease, which presents certain difficulties in treatment. Chemotherapy and targeted therapy can control esophageal cancer to some extent, but some patients may develop drug resistance, leading to decreased therapeutic effect. For patients with advanced esophageal cancer, the efficacy of current treatments is limited, and more effective therapeutic strategies need to be explored. Therefore, through in-depth research on the mechanisms of the development of ESCC and screening for prognostic biomarkers, it can provide more precise guidance for personalized treatment, which will help improve patient prognosis and enhance treatment effectiveness as well as quality of life.

Deubiquitinating enzymes (DUBs) are a class of enzymes that can hydrolyze the linkage of ubiquitin proteins, reversing the action of the ubiquitin-proteasome system, thereby regulating the stability and activity of intracellular proteins (6, 7). According to the differences in their catalytic domains, DUBs can be divided into several categories: ubiquitin-specific proteases (USPs), carboxyl-terminal hydrolases (UCHs), ovarian tumor proteases (OTUs), Machado–Josephin domain proteases, JAB1/MPN/MOV34 proteases, monocyte chemotactic protein–induced proteins, the novel motif interacting with ubiquitin-containing DUB family, and Zinc finger with UFM1-specific peptidase domain protein, among which USPs are the most numerous category (8–10). In tumor cells, abnormal expression or dysfunction of some DUBs is closely related to the occurrence, development, and treatment resistance of tumors (8). USP38 belongs to the USPs subfamily of DUBs and plays an important regulatory role in inflammatory responses, antiviral infection, cell proliferation, migration, invasion, DNA

‡ These authors contributed equally to this work.
* For correspondence: Jiancai Tang, tangjiancai@nsmc.edu.cn; Qingyong Hu, huqy@nsmc.edu.cn.

damage repair, and chemotherapy resistance (11–18). Much evidence indicates that USP38 acts in a context-dependent manner in tumors. For instance, USP38 promotes the progression of gastric cancer and lung cancer (13, 14), while inhibiting the progression of clear cell renal carcinoma, colorectal cancer, and bladder cancer (15–18). However, the role of USP38 in ESCC is still unclear. The known direct substrates of USP38 include HDAC1, HDAC3, HMX3, JunB, HIF1α, TBK1, and fatty acid synthase (13, 15–17, 19–21). Although many substrates of USP38 have been identified, few upstream regulatory factors of USP38 have been identified.

ADAR1 (ADAR) is a member of the adenosine deaminases acting on RNA family, containing two isoforms: the interferon (IFN)-inducible p150 isoform and the constitutively expressed p110 isoform (the isoform involved in this study is p110, referred to collectively as ADAR). The p150 isoform is subcellularly localized in both the nucleus and cytoplasm, whereas p110 is primarily localized in the nucleus (22, 23). The p110 isoform contains a Zβ domain associated with Z-DNA/Z-RNA binding, three dsRNA-binding domains, and deaminase domains, while p150 has an additional Z-DNA/Z-RNA binding Zα domain at the N terminus compared to p110 (24). The classical function of ADAR is RNA editing, which involves converting adenosine (A) in RNA to inosine (I), affecting RNA stability, translation, miRNA-mediated gene silencing, and the ability to be recognized by innate immune sensors (25, 26). Initially, researchers confirmed that ADAR plays a crucial role in the IFN signaling pathway–mediated antiviral immune response, where IFN can induce ADAR expression, and ADAR can inhibit RIG-I–like receptor signal activation through RNA editing to achieve a negative feedback regulation of the antiviral effects (27). However, recent studies have shown that ADAR is highly expressed in various tumors and promotes their progression, including ESCC, non–small cell lung cancer, colorectal cancer, and breast cancer (28–31). In particular, the overexpression of ADAR in ESCC leads to excessive A-to-I editing of the AZIN1 messenger RNA, which gives it the function of promoting malignant progression (28). With in-depth research on ADAR, researchers have found that ADAR possesses functions independent of RNA editing (23). However, the role of ADAR in ESCC, independent of its RNA editing function, remains still unclear.

In this study, we demonstrated that USP38, acting as an oncogene, plays a significant role in the proliferation and growth of ESCC cells. Mechanistically, ADAR interacts with USP38 to enhance USP38 protein stability and promote USP38 auto-deubiquitylation. These results highlight the potential of targeting the ADAR–USP38 axis for the treatment of ESCC.

Results

Knockdown of USP38 inhibits ESCC growth

DUBs stabilize their substrates by removing ubiquitin chains from them. The largest DUB subfamily is the USPs, which contains 57 members (32). To explore the deubiquitinases that play a significant role in esophageal cancer, we first analyzed differentially expressed genes *via* GEPIA (http://gepia.cancer-pku.cn/index.html). We found that, under default conditions (log2FC cut-off of 1, q-value cut-off of 0.01), there were ten deubiquitinases among the differentially expressed genes, with seven upregulated (USP38, USP42, USP18, USP10, USP9X, USP14, and USP13) and three downregulated (USP2, USP32P1, and USP9Y) (Fig. 1*A*). Compared to normal tissues, USP38 was the most significantly upregulated in esophageal cancer tissues (Fig. 1, *A* and *B*). USP38 was significantly overexpressed in both esophageal adenocarcinoma and squamous cell carcinoma tissues compared to normal tissues (Fig. 1*C*). Furthermore, ESCC patients with elevated USP38 expression exhibit a poorer recurrence-free survival (Fig. S1). Additionally, there have been no reports on the role of USP38 in esophageal cancer. We hypothesized that it may play an important role in the development of esophageal cancer. Therefore, we knocked down USP38 in two esophageal squamous cell lines and found that knockdown of USP38 significantly inhibited the growth of esophageal squamous cells through Cell Counting Kit-8 (CCK-8) and colony formation analysis (Fig. 1, *D*–*F*). To further clarify the role of USP38 in the growth of ESCC, we analyzed the effect of USP38 on the *in vivo* growth of ESCC cells using the CDX model. The results showed that knockdown of USP38 inhibited tumor growth in the Eca-109 xenograft mouse model (Fig. 1, *G*–*I*). Together, these results indicate that USP38 plays an important role in the proliferation of ESCC cells and the growth of ESCC.

USP38 stabilizes itself through auto-deubiquitylation

Previous results showed that USP38 is highly expressed in ESCC (Fig. 1*C*). Thus, we asked ourselves why USP38 would be upregulated in ESCC. Considering that deubiquitinases inherently function as hydrolases, their mechanism of action relies on the interaction between the enzyme and its substrates. Previous studies have reported that some deubiquitinases can stabilize themselves through auto-deubiquitylation (33). Based on this, we first analyzed proteins interacting with USP38 through the protein interaction database BioGRID (https://thebiogrid.org/), where we discovered that USP38 is one of its own interacting proteins. We speculated that USP38 may form homologous dimers to execute its function or USP38 is its own substrate. Here, we introduced two mutants of USP38, USP38 C454A and the double mutant USP38 C454A/H857A, to render USP38 enzymatically inactive. Indeed, through immunoprecipitation (IP) analysis of the interaction between HA-tagged or Flag-tagged USP38 WT with mutants, we found that USP38 exhibits homomeric interaction, and this intermolecular interaction does not depend on its enzymatic activity (Fig. 2, *A* and *B*). Further, we hypothesized that loss of USP38 catalytic activity might lead to its enhanced ubiquitination. Therefore, we analyzed the ubiquitination levels of Flag-USP38 WT and Flag-USP38 C454A/H857A by coexpressing them with His-tagged ubiquitin (His-Ub) respectively and immunoprecipitating ubiquitylated proteins with a His antibody. The results showed that His-Ub retrieved more USP38 C454A/H857A while little WT

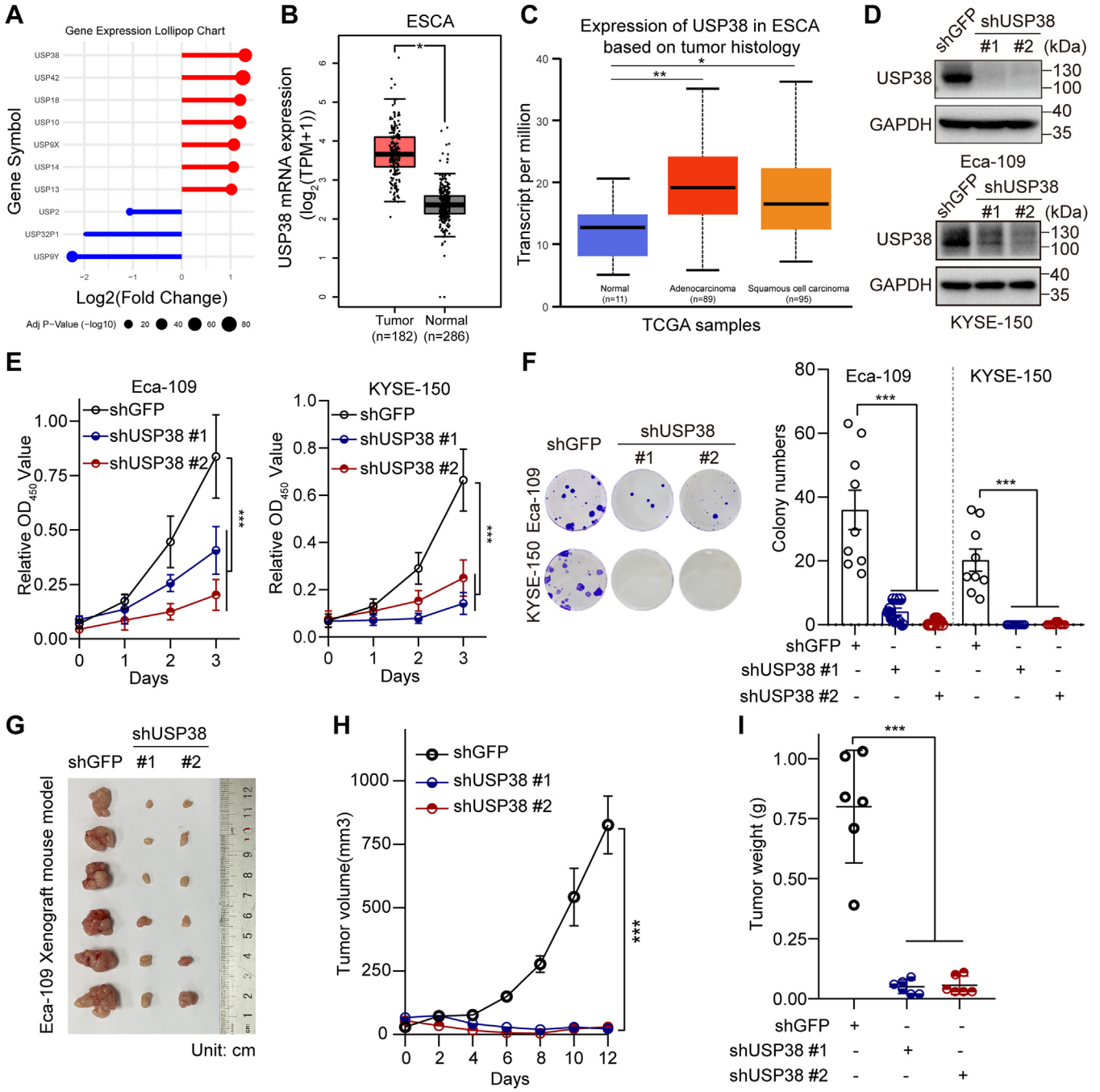

Figure 1. Knockdown of USP38 inhibits esophageal squamous cell carcinoma cells proliferation and growth *in vitro* and *in vivo*. *A*, the lollipop plot shows the differentially expressed deubiquitinases in esophageal cancer based on the GEPIA database. *B*, analysis of USP38 mRNA expression levels in normal tissues and esophageal cancer tissues *via* the GEPIA database. *C*, analysis of USP38 mRNA expression levels in normal tissues, esophageal adenocarcinoma tissues, and squamous cell carcinoma tissues was conducted using the UALCAN database (https://ualcan.path.uab.edu/index.html). *D-F*, Eca-109 and KYSE-150 cells with stable expression of shGFP, shUSP38 #1, or shUSP38 #2 were generated and subjected to Western blot analysis (*D*), CCK-8 assay (*E*), or colony formation assay (*F*). Three independent experiments were performed. Data are presented as mean ± SD. *G–I*, Eca-109 stable cells (1×10^6/mices), as indicated, were subcutaneously injected into the flanks of 5-week-old female BALB/c nude mice (n = 6/group). Tumor sizes were measured every other day. Mice were sacrificed on day 12, tumors were excised and photographed. Tumor volume and tumor weight were presented as mean ± SEM. Comparisons were performed with two-way ANOVA with Bonferroni's test (*E*, *H*) and one-way ANOVA with Bonferroni's test (*F*, *I*). *$p < 0.05$, **$p < 0.01$, and ***$p < 0.001$. CCK-8, Cell Counting Kit-8; USP, ubiquitin-specific protease.

USP38 was pulled down (Fig. 2*C*). To further clarify that USP38 can indeed regulate its own ubiquitination level, we coexpressed WT USP38 (Flag-USP38 WT) and two inactive mutants (Flag-USP38 C454A or C454A/H857A) with His-Ub, respectively, followed by IP analysis using Flag antibody. The results showed that compared to USP38 WT, the ubiquitination levels of USP38 C454A and C454A/H857A were significantly increased (Fig. 2*D*). Together, these results indicate that USP38 regulates its own ubiquitination level in an enzyme activity–dependent manner.

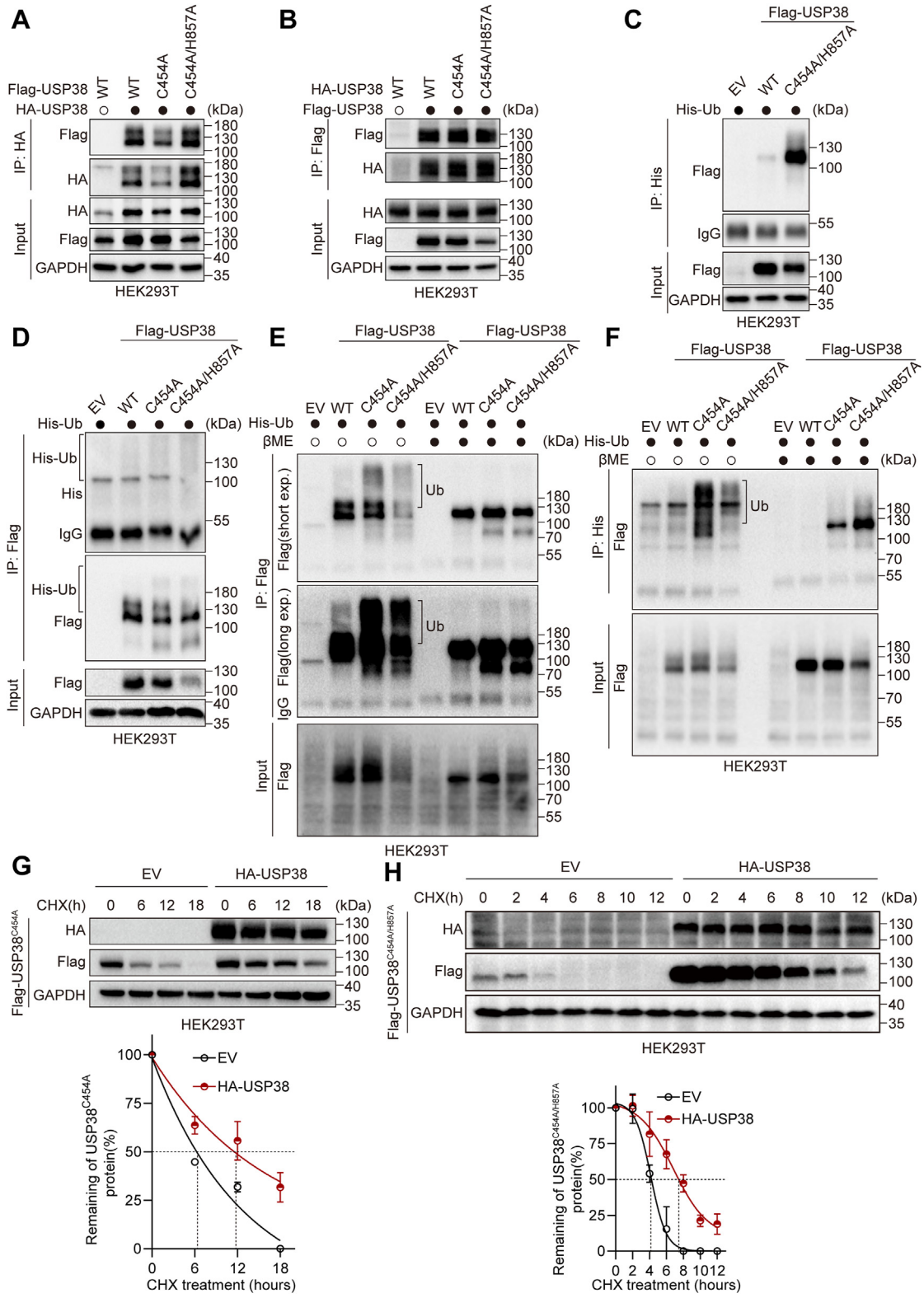

Figure 2. USP38 stabilizes itself through auto-deubiquitylation. *A* and *B*, HEK293T cells expressing Flag-USP38 (WT, C454A, C454A/H857A) and HA-USP38 or HA-USP38 (WT, C454A, C454A/H857A) and Flag-USP38 (as shown in the plasmids) for 48 h. Cells were treated with MG132 for 6 h before immunoprecipitation and Western blot analysis. *C* and *D*, HEK293T-His-Ub cells expressing Flag-USP38 (WT, C454A, or C454A/H857A) for 48 h, followed by immunoprecipitation analysis using His antibody or Flag antibody conjugated beads, then Western blot analysis to detect the indicated proteins. *E* and *F*, HEK293T-His-Ub cells expressing Flag-USP38 (WT, C454A, or C454A/H857A) for 48 h, followed by immunoprecipitation analysis using His antibody or Flag antibody conjugated beads in the presence or absence of β-mercaptoethanol (β-ME), then Western blot analysis to detect the proteins as shown (exp., exposure). *G* and *H*, HEK293T cells expressing Flag-USP38 (C454A or C454A/H857A) were transfected with HA-USP38 or EV (empty vector) for 48 h. Cells were then treated with 50μg/ml cycloheximide (CHX) for the indicated time intervals. Cell lysates were used for Western blot analysis. The plots of USP38 (C454A or C454A/H857A) protein half-life were presented as mean ± SEM (n = 3 biologically independent samples). His-Ub, His-tagged ubiquitin; USP, ubiquitin-specific protease.

Previous studies have shown that USP4 can undergo auto-deubiquitylation, and ubiquitination modifications occur on the cysteine residues of USP4 in a covalent-binding manner (33). Therefore, we questioned whether USP38 also has a similar ubiquitylation modification on its cysteine residues. It has been reported that the reducing agent β-mercaptoethanol (β-ME) can disrupt cysteine ubiquitylation (33). Based on this, we analyzed whether the ubiquitylation of USP38 is sensitive to β-ME treatment. Thus, we used a Flag antibody for IP analysis to analyze the ubiquitination modification of USP38 in the absence or presence of β-ME, and we found that the ubiquitylation modification of USP38 C454A and C454A/H857A dramatically increased, which was lost upon β-ME treatment (Fig. 2*E*). Simultaneously, we also noted that USP38 WT had similar cysteine ubiquitylation modifications to a lesser extent than the inactive mutants (Fig. 2*E*). To further clarify this finding, we performed IP analysis with His-Ub, followed by Western blot analysis using an antibody recognizing Flag, showing that the ubiquitination modification of USP38 C454A and C454A/H857A also increased, and these modifications could not be observed after β-ME treatment (Fig. 2*F*). These results indicate that the ubiquitinated USP38 C454A and C454A/H857A are sensitive to the reducing agents, which also indicates that the protein is subject to cysteine ubiquitination modification. USP38 C454A and C454A/H857A are more prone to ubiquitylation modifications, and ubiquitylation is a signal marker for protein degradation. Based on the above results, we asked whether USP38 WT can stabilize the protein levels of USP38 C454A or C454A/H857A. We analyzed the protein stability using cycloheximide treatment on cells and found that, compared to the control, USP38 WT enhanced the protein stability of USP38 C454A and C454A/H857A (Fig. 2, *G* and *H*). Together, these findings indicate that USP38 counteracted its own ubiquitylation, thereby enhancing its stability.

ADAR enhances the stability of USP38 protein

To further explore the reasons for the stability of USP38 protein, we identified proteins interacting with USP38 through IP-mass spectrometry analysis. Our mass spectrometry results showed that, in addition to USP38 itself being highly enriched, the number of unique peptides and coverage of ADAR were the highest, at 37 and 31%, respectively (Fig. 3*A*). ADAR is an enzyme involved in RNA editing, capable of converting adenosine (A) on RNA to inosine (I), affecting RNA stability and coding capacity, thereby regulating gene expression. The role of ADAR in ESCC is not limited to its RNA editing activity. Studies have also found that ADAR may affect tumor development and patient survival through mechanisms other than RNA editing, such as interaction with other proteins (23). To further confirm the interaction between USP38 and ADAR, we coexpressed USP38 and ADAR proteins tagged with different tags in HEK293T cells and then analyzed the interaction between USP38 and ADAR through IP. The results showed that USP38 and ADAR proteins could pull each other down (Fig. S3, *A* and *B*). Endogenous coimmunoprecipitation results also showed that stable protein complexes between ADAR and USP38 were readily detected (Fig. 3, *B* and *C*). Furthermore, we analyzed the colocalization of USP38 and ADAR by immunofluorescence and found that both heterologously coexpressed ADAR-HA and Flag-USP38, as well as endogenous ADAR and USP38, were localized in the nucleus, with a strong colocalization fluorescence intensity observed (Fig. 3*D*). The results of nucleo-cytoplasmic separation also indicated that overexpression of ADAR enhanced the accumulation of USP38 in the nucleus (Fig. 3*E*). These results indicate that USP38 and ADAR interact in the cell nucleus. Based on this, we hypothesized that there is a regulatory relationship between USP38 and ADAR. Considering that USP38 is a DUB, we speculated that ADAR may be a direct substrate of USP38. Therefore, we first knocked down USP38 in two ESCC cell lines, Eca-109 and KYSE150, and then detected changes in ADAR protein levels through Western blotting, finding that USP38 does not affect ADAR protein expression (Fig. S2). Further, we knocked down or overexpressed ADAR in Eca-109 and KYSE150, respectively, and then performed Western blot analysis. We found that knocking down ADAR inhibited USP38 protein expression, while overexpressing ADAR promoted USP38 protein expression (Fig. 3, *F* and *G*). Next, we analyzed the effect of ADAR on USP38 mRNA expression levels by real-time quantitative PCR (qPCR), and the results showed that ADAR had no effect on USP38 mRNA expression levels (Fig. S3, *C* and *D*). Based on the above results, we speculated that ADAR may regulate USP38 protein levels by regulating USP38 protein stability. Indeed, protein stability analysis results showed that, compared to control, overexpression of ADAR enhanced USP38 protein stability (Fig. 3*H*). Previous results showed that USP38 can stabilize itself through auto-deubiquitylation (Fig. 2). We asked whether ADAR also plays a role in the auto-deubiquitylation of USP38. We analyzed the effect of overexpressing ADAR on the auto-deubiquitylation of USP38 through IP, and the results showed that overexpressing ADAR reduced the ubiquitination of USP38 C454A (Fig. 3*I*). These results indicate that ADAR promotes the auto-deubiquitylation of USP38 and thereby stabilizes USP38 through interaction with USP38.

The interaction between USP38 and ADAR depends on its enzymatic active region

To clarify the structural domains involved in the USP38 and ADAR interaction, a series of deletion mutants of USP38 (WT (1-1042AA), N-term (1-400AA), C-term (401-1042AA)) and ADAR (WT (1-931AA), ΔZD (deletion of 1-71AA), ΔRBD (deletion of 207-499AA), and ΔDD (deletion of 591-926AA)) were used for IP analyses. The IP results of ADAR WT and its deletion mutants coexpressed with USP38 WT indicated that the deaminase domain domain (amino acids 591–926) of ADAR is required for interacting with USP38 (Fig. 4, *A* and *B*). Additionally, IP assays using truncated mutants of USP38 and ADAR WT indicated that the USP domain of USP38 is necessary for binding to ADAR (Fig. 4, *C* and *D*).

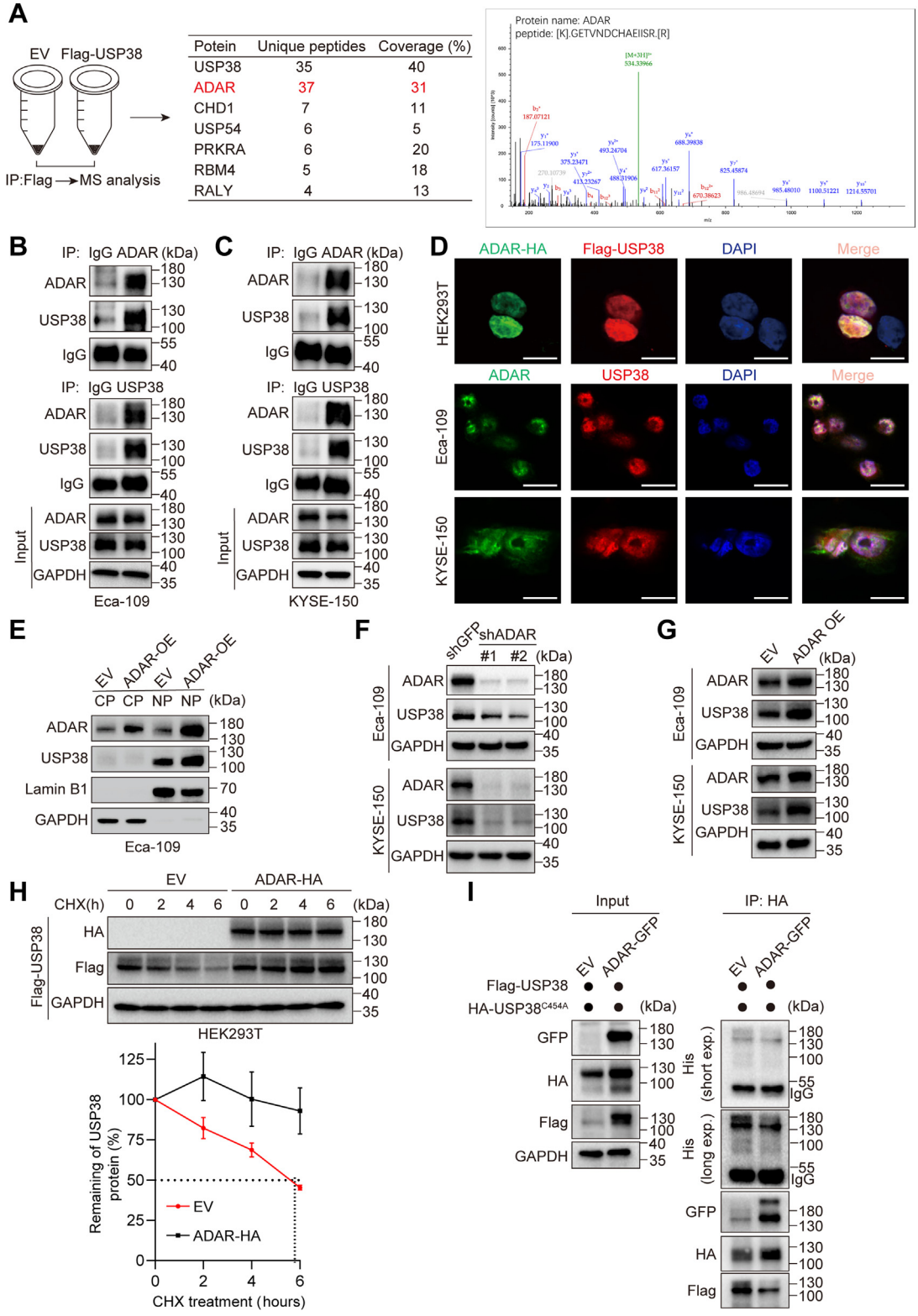

Figure 3. ADAR stabilizes USP38. *A*, HEK-293T cells expressing EV (empty vector) or Flag-USP38 for 48 h, then immunoprecipitation was performed using Flag antibody conjugated beads, and the pulled down proteins were identified by mass spectrometry analysis. *B* and *C*, Eca-109 or KYSE-150 cells were subjected to coimmunoprecipitation (co-IP) with specific antibodies against USP38 or ADAR, or with an IgG control, followed by Western blot analysis. *D*, HEK293T cells coexpressing Flag-USP38 and ADAR-HA, along with Eca-109 or KYSE-150 cells, were subjected to immunofluorescence staining to assess the colocalization of USP38 and ADAR. The scale bar represents 20 μm. *E*, Eca-109 cells stably expressing ADAR or EV (empty vector) were subjected to cellular fractionation, followed by Western blot analysis of ADAR and USP38 expression in cytoplasm and nucleus. *F* and *G*, Eca-109 or KYSE-150 cells stably expressing shADAR (#1 or #2), ADAR, or control were subjected to Western blot analyses. *H*, HEK-293T cells co-expressing Flag-USP38 and EV (empty vector) or ADAR-HA for 48 h, followed by treatment with 50μg/ml cycloheximide (CHX) for an indicated time interval. Cell lysates were used for Western blot analysis. The plots of USP38 protein half-life were presented as mean ± SEM (n = 3 biologically independent samples). *I*, HEK293T cells expressing His-Ub

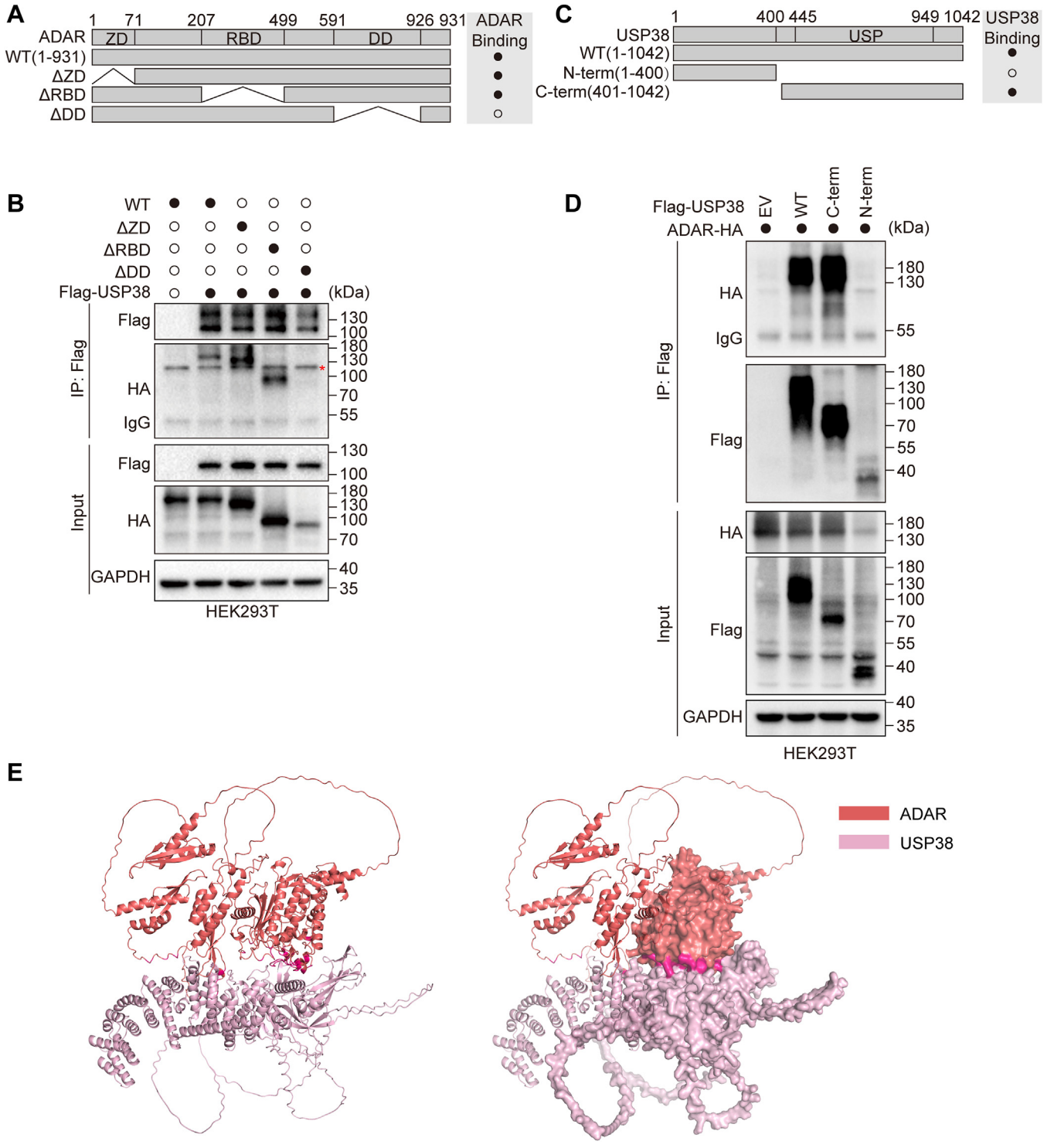

Figure 4. USP38 interacts with ADAR. *A*, schematic diagram of ADAR deletion mutants. The ability of ADAR deletion mutants to bind USP38 is indicated (•, binding; ○, no binding). *B*, HEK293T cells were cotransfected with Flag-USP38 and different ADAR mutants (WT, ΔZD, ΔRBD, or ΔDD) for 48 h. After treating the cells with MG132 for 6 h, immunoprecipitation was performed using Flag antibody, followed by Western blot analysis of the indicated proteins. *C*, schematic representation of USP38 truncation mutants. The ability of USP38 truncation mutants to bind ADAR is indicated (•, binding; ○, no binding). *D*, HEK293T cells were cotransfected with ADAR-HA and different USP38 mutants (WT, C-term, or N-term) for 48 h. After treating the cells with MG132 for 6 h, cell lysates were immunoprecipitated, followed by Western blot analysis. *E*, the structure of the ADAR and USP38 complex was predicted using DMFold (https://zhanggroup.org/DMFold/). The full-length USP38 and ADAR were shown as *light pink* and *deep salmon cartoons*, respectively. The USP domain of USP38 and the DD domain (deaminase domain) of ADAR were displayed as surfaces. The interface of the interaction between USP38 and ADAR was shown in *hot pink*. ADAR, adenosine deaminase acting on RNA; RBD, RNA-binding domain; USP, ubiquitin-specific protease; ZD, Zβ domain.

were transfected with the plasmids as shown for 48 h, followed by immunoprecipitation analysis with HA antibody–conjugated magnetic beads, then Western blot analysis of the proteins as shown. ADAR, adenosine deaminase acting on RNA; CP, cytoplasm protein; His-Ub, His-tagged ubiquitin; IgG, immunoglobulin G; NP, nucleolus protein; USP, ubiquitin-specific protease.

Subsequently, we used the online web tool DMFold (https://zhanggroup.org/DMFold/) to predict the structure of the USP38 and ADAR complex. DMFold (also known as DMFold-multimer) is a deep learning–based approach to protein complex structure and function prediction built on deep multiple sequence alignments. The core of the pipeline is the integration of deep multiple sequence alignment 2 with the modified structure module of AlphaFold2 (34). DMFold predicted five structures for the USP38–ADAR complex. The top three ranked structures—TOP1 (Fig. 4*E*), TOP2 (Fig. S4*A*), and TOP3 (Fig. S4*B*)—all demonstrated interactions between the USP domain of USP38 and the deaminase domain domain of ADAR, consistent with our IP experiment results (Fig. 4, *A*–*D*). These findings demonstrate that the interaction between USP38 and ADAR is mediated through their C-terminal enzymatic catalytic regions.

ADAR inhibition of ESCC cells proliferation depends on USP38

Previous research results show that USP38 is one of the binding proteins of ADAR. ADAR can enhance the protein stability of USP38 and upregulate USP38. To further clarify the role of USP38 in ADAR-mediated proliferation of ESCC cells, we performed rescue experiments by knocking down ADAR while overexpressing USP38 in two esophageal squamous carcinoma cell lines, Eca-109 and KYSE-150. The results showed that knocking down ADAR downregulated the expression of USP38 and c-Myc, and overexpressing USP38 reversed the changes in c-Myc expression mediated by knocking down ADAR in Eca-109 and KYSE-150 cells, with c-Myc being a downstream effector of USP38 (Fig. 5*A*). We then detected whether USP38 could rescue the inhibitory effect of ADAR knockdown on esophageal squamous carcinoma cells proliferation through CCK-8 and colony formation assays. Consistently, both CCK-8 and colony formation assay results indicated that knocking down ADAR inhibited Eca-109 and KYSE-150 esophageal squamous carcinoma cells proliferation, while restoring USP38 expression reversed the inhibitory effect on cells proliferation caused by knocking down ADAR (Fig. 5, *B* and *C*). These results demonstrate that USP38 plays a causative role in ADAR-mediated esophageal squamous carcinoma cells proliferation.

Discussion

The substrate specificity of DUBs makes them potential therapeutic targets. As a member of the deubiquitinase family, the role of USP38 in tumors remains controversial, whether it is tumor suppressive or oncogenic that varies across different cancers. It has been reported that USP38 promotes gastric cancer progression by upregulating fatty acid synthase (13). In addition, USP38 promotes lung cancer cell proliferation by stabilizing c-Myc (14). These evidences support the oncogenic role of USP38 in cancers. Conversely, some studies also suggest USP38 as a tumor suppressor, such as USP38 promotes nonhomologous end joining repair in kidney clear cell carcinoma cancer by deubiquitinating HDAC1 to modulate its activity, maintaining genome stability and regulating cancer cells' response to genotoxic insults (15); USP38 inhibits tumor stemness in colorectal cancer by mediating K63 deubiquitination of HDAC3 (16); USP38 suppresses cell proliferation and migration by downregulating HMX3 ubiquitination in colorectal cancer (17); METTL14 inhibits bladder cancer cell migration and invasion by stabilizing USP38 (18). In this study, we show that silencing USP38 inhibits ESCC cell proliferation and growth *in vitro* and *in vivo*. Mechanistically, we demonstrate that ADAR enhances USP38 auto-deubiquitylation to increase USP38 protein stability and upregulate USP38, thereby affecting cell proliferation and growth. Our study supports the oncogenic role of USP38 in ESCC. Therefore, when targeting USP38 as a therapeutic target, we need to fully understand its specific role in the context of specific tumors.

DUBs interact with their substrates, specifically recognizing substrates and removing ubiquitin chains from them. Researchers have found that DUBs are also regulated by themselves, meaning that the same DUB molecule acts as both the "executor" and "executee" in the deubiquitination process. This process is defined as "auto-deubiquitylation" (33). DUBs can self-regulate through either intermolecular or intramolecular mechanisms (35). In this study, USP38 demonstrates homomeric interactions, indicating that it regulates its own protein levels *via* intermolecular auto-deubiquitylation. Existing studies have shown that auto-deubiquitylation of USP4 enhances its interaction with CtIP/MRN, thereby promoting homologous recombination (33). Similarly, like USP4, the catalytically inactive USP15 shows impaired binding to its target proteins SMAD2/3 (33). These evidences provide an important mechanism of action, where the auto-deubiquitylation of deubiquitinases can promote their interaction with substrates, thereby affecting downstream proteins and signaling pathways. In this study, we found that, similar to the auto-deubiquitylation of USP4 and USP15, USP38 can enhance its own stability through auto-deubiquitylation. We mentioned earlier studies reporting that in addition to regulating tumor cell proliferation, growth, migration, and invasion, USP38 is also involved in regulating DNA damage repair and inflammation. Whether stress conditions such as DNA damage and inflammation would affect the auto-deubiquitylation of USP38 and thus alter its interaction patterns with substrates is worth further exploration. The ubiquitination modifications we know generally occur on the lysine residues of substrates, and different types of ubiquitin chain modifications on substrate lysine residues produce different biological functions. Currently, eight different types of ubiquitin modifications have been identified, including K6, K11, K27, K29, K33, K48, K63, and Met1 (36). Previous studies have shown that USP38 can recognize various types of ubiquitin modifications, including K11 (20), K27 (11), K33 (21, 37), K48 (19, 21, 37), and K63 (15, 16). It is noteworthy that USP38 can simultaneously recognize and remove both K33 and K48 types of ubiquitin chain modifications. These are referred to as classical ubiquitination modifications, compared to which, ubiquitination modifications on cysteine residues have been less studied. We found that the ubiquitination modification of USP38 is sensitive to the reducing agent β-ME, indicating the

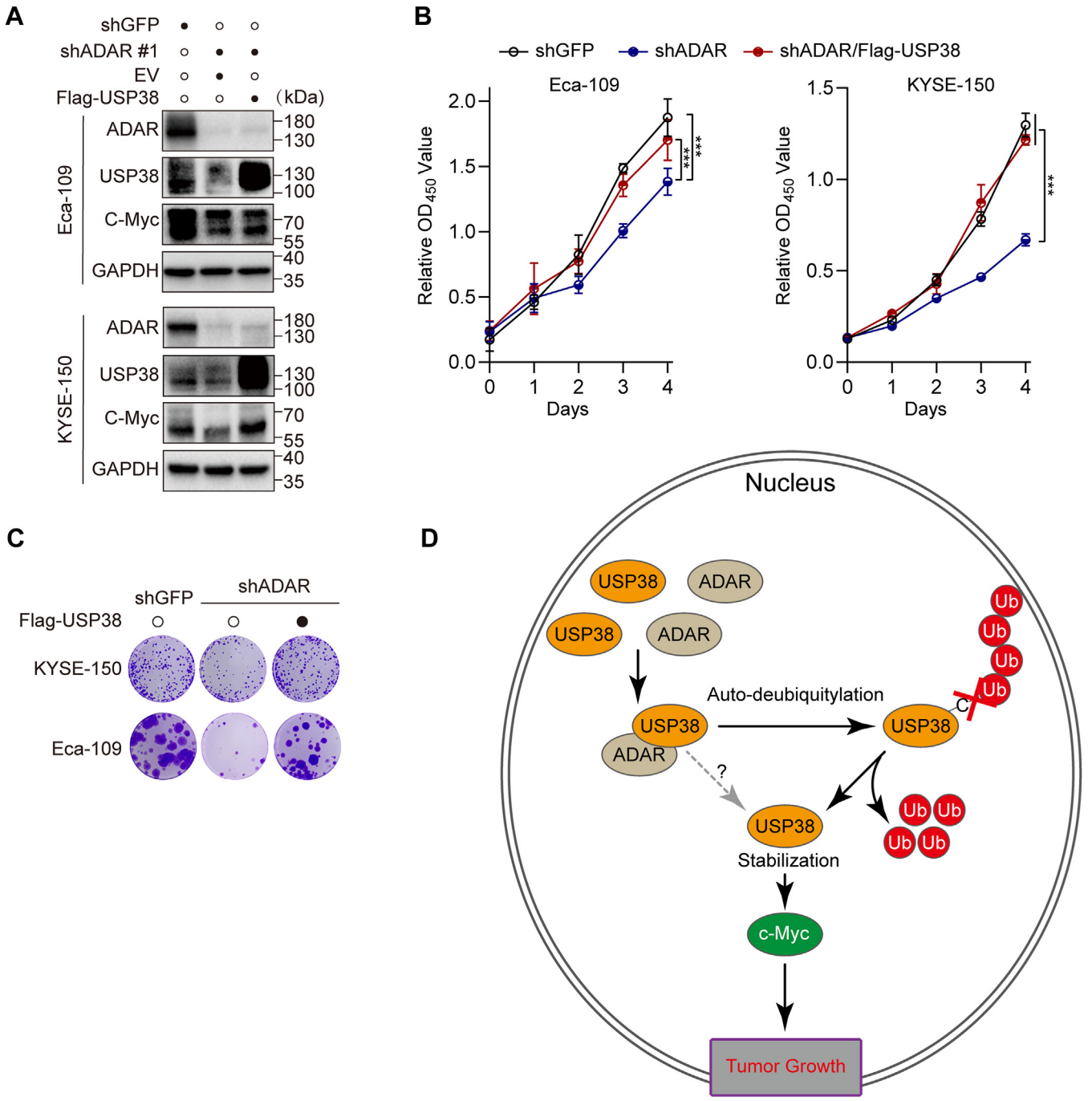

Figure 5. ADAR regulates esophageal squamous cell carcinoma cells proliferation through USP38. *A-C*, Eca-109 or KYSE-150 cells stably expressing shADAR, or both Flag-USP38 and shADAR were subjected to Western blot analyses (*A*), CCK-8 assays (*B*), or colony formation analyses (*C*). Data from three independent repeat experiments are presented as mean ± SD. *D*, a working model depicts that ADAR promotes USP38 auto-deubiquitylation and stability to regulate esophageal squamous cell carcinoma cells growth. Comparisons were performed with two-way ANOVA with Bonferroni's test (*B*). *$p < 0.05$, **$p < 0.01$, and ***$p < 0.001$. ADAR, adenosine deaminase acting on RNA; CCK-8, Cell Counting Kit-8; USP, ubiquitin-specific protease.

presence of covalent ubiquitination modifications on cysteine residues of USP38. Whether different types of ubiquitination modifications also exist on cysteine residues remains to be explored. In this study, catalytically inactive USP38 (USP38 C454A and C454A/H857A) was unstable, while the USP38 WT could stabilize USP38 C454A and C454A/H857A. We reasonably speculated that ubiquitination modifications on cysteine residues, similar to classic ubiquitination modifications, mediate its degradation. Apart from the catalytic center's cysteine residue being crucial for the hydrolytic activity of the USPs subfamily of deubiquitinases, modifications on other cysteine residues also regulate their fate. Our laboratory research found that $KRAS^{G12V}$ promotes the stability and activation of USP5 through reactive oxygen species-induced homodimer formation *via* disulfide bonds at C195 (13). These evidences suggest that modifications on cysteine

residues, including cysteine ubiquitination, might be widespread, but the functional changes caused by these modifications require further in-depth study.

The ADAR family contains three members: ADAR1 (ADAR), ADAR2 (ADARB1), and ADAR3 (ADARB2), which alter RNA molecules through A-to-I editing, affecting the function of both coding and noncoding RNAs. The RNA editing activities of ADAR and ADAR2 are known to be involved in various biological processes, while the function of ADAR3 remains unclear (23). In tumors, the canonical RNA editing functions of ADAR include direct editing on mRNAs and noncoding RNAs, which can alter protein functions or regulate the actions of noncoding RNAs, thereby influencing tumor development (23, 38). In ESCC, high expression of ADAR drives its development, and poor prognosis is positively correlated. Mechanistically, ADAR promotes the proliferation and invasion of tumor cells through editing the mRNA of AZIN1 to confer an acquired function (28). Similarly, in colorectal cancer, ADAR-driven A-to-I RNA-edited AZIN1 upregulates interleukin-8 to promote tumor angiogenesis (30). However, recent studies have shown that ADAR also plays an important regulatory role in tumors independent of its RNA editing function (23, 39). For example, it has been reported that ADAR inhibits the formation of the DGCR8–DROSHA complex by interacting with DGCR8, suppressing the maturation of miRNAs (40). Furthermore, ADAR promotes the ubiquitination and degradation of DROSHA by interacting with it (41). Besides the protein–protein interaction mode of ADAR that is independent of its RNA editing function, some studies have reported that ADAR can act as an RNA-binding protein to directly exert regulatory effects on RNAs independent of its editing function (23). The regulation of DUBs activity involves various mechanisms, including conformational rearrangement of the catalytic triad, enhancement of enzyme activity by partner proteins, and auto-inhibitory homotetramer formation (10, 42). Studies have shown that UCHL1 and USP7 can remodel enzyme activity through conformational rearrangements (43–45). Furthermore, the UCHL1 R178Q mutant, identified in patients with early-onset neurodegenerative diseases, exhibits higher catalytic activity than the UCHL1 WT. This increased enzymatic activity of UCHL1 R178Q is due to its higher K_{cat} value (46). In this study, we demonstrate that ADAR enhances the auto-deubiquitylation and stabilization of USP38. Structural predictions suggest that ADAR and USP38 interact within their enzymatic activity domains, raising the question of whether ADAR induces conformational changes in USP38 to modulate its enzymatic activity. The precise mechanism by which ADAR regulates USP38 enzymatic activity requires further investigation. In conclusion, we show that ADAR enhances USP38 protein stability by interacting with it, and overexpression of USP38 rescues the inhibitory effect of ADAR knockdown on ESCC cell proliferation. Mechanistically, ADAR stabilizes USP38 by enhancing its auto-deubiquitylation. Our study further confirms the important role of ADAR in regulating USP38 in esophageal squamous carcinoma in a manner independent of its RNA editing function. More importantly, our results provide a rationale for targeting the ADAR–USP38 axis for the treatment of ESCC.

Experimental procedures

Cell culture

Eca-109 and HEK-293T cells were cultured in Dulbecco's modified Eagle's medium (GIBCO), while KYSE-150 cells were in RPMI 1640 medium (GIBCO), both supplemented with 10% fetal bovine serum (C04001, Biological Industries) and 1% penicillin/streptomycin/amphotericin B solution (P7630, Solarbio). All cell lines, sourced from the National Collection of Authenticated Cell Cultures of China and routinely tested for *mycoplasma* contamination, were maintained at 37 °C in a 5% CO_2 humidified atmosphere.

Plasmid transfection, lentiviral infection, and RNAi

Cells were transfected at 70 to 80% confluence using polyethyleneimine (24765-100, Polysciences). The following expression plasmids were used: Human Flag-USP38, Flag-USP38^{C454A}, Flag-USP38$^{C454A/H857A}$, Flag-USP38N-term (1-400AA), Flag-USP38C-term (401-1042AA), HA-USP38, HA-USP38^{C454A}, HA-USP38$^{C454A/H857A}$, ADAR-HA, ADAR-HA$^{\triangle ZD}$, ADAR-HA$^{\triangle RBD}$, ADAR-HA$^{\triangle DD}$, GFP-ADAR, and His-Ub. Recombinant lentiviruses were produced by cotransfecting HEK-293T cells with pMD2.G, psPAX2 packaging plasmids, and the lentiviral expression plasmid using polyethyleneimine. Viral particles were collected at 48 h posttransfection and concentrated *via* ultracentrifugation. For lentiviral infection, cells at 35% confluence were infected with recombinant lentivirus or an empty vector (EV) control. Infection was facilitated by 10μg/ml polybrene and followed by a 48-h incubation at 37 °C with 5% CO_2. Puromycin selection was applied for an additional 48 h postinfection. For RNAi, lentiviral-based shRNAs targeting USP38, ADAR, or GFP were cloned into the pLKO.1-puromycin vector. Primer sequences for these shRNAs are detailed in Table S1.

Western blot analyses

For Western blot analysis, cellular samples were harvested, washed with cold PBS, and lysed using Western and IP cell lysis buffer (Beyotime, P0013) supplemented with the proteasome inhibitor PMSF (Beyotime, ST507). Equivalent amounts of protein were loaded, resolved by SDS-PAGE, and then transferred onto polyvinylidene fluoride membranes (Millipore, ISEQ00010). The membranes were blocked with 5% nonfat dry milk before being incubated with primary antibodies, followed by detection with horseradish peroxidase–conjugated secondary antibodies for chemiluminescent detection (Bio-Rad ChemiDoc XRS+, Bio-Rad). Image Lab Software 6.1 (https://www.bio-rad.com/zh-cn/product/image-lab-software) was employed for gel and blot images analysis. The antibodies targeted USP38 (Proteintech, 17767-1-AP, 1:1000), ADAR1 (Abways, CY8635, 1:1000), GAPDH (Abways, AB0037, 1:5000), GFP (Proteintech, 66002-1-Ig, 1:20,000), Flag

(Cell Signaling Technology, 14793S, 1:1000), HA (Proteintech, 66006-2-Ig, 1:10,000), Ubiquitin (Affinity, BF8034, 1:1000), His (ZENBIO, 230,001, 1:5000), c-Myc (Cell Signaling Technology, #5605, 1:1000), Lamin B1 (Abways, AB0054, 1:5000), and horseradish peroxidase–conjugated secondary antibodies against mouse (Abways, AB0102, 1:5000) and rabbit (Affinity, S0001, 1:3000).

IP, mass spectrometry, and ubiquitylation assays

For exogenous IP, cells were collected, washed once with cold PBS, and lysed using Western and IP cell lysate buffer (Beyotime, P0013) with proteasome inhibitor PMSF (Beyotime, ST507). The cells were lysed gently for 30 min on ice, vortexed, and shaken every 10 min, then centrifuged at 12,000×*g* for 30 min. After protein quantification, input was prepared. Equal amounts of total protein were incubated overnight with anti-HA beads or anti-Flag beads. The beads were then washed three times with Western and IP cell lysate buffer. Prior to Western blot analysis, the beads were heated at 100 °C for 8 min. The following reagents were used in this study: anti-Flag Magnetic Beads, anti-HA magnetic beads, and protein A/G magnetic beads (MCE).

For endogenous coimmunoprecipitation, cells were harvested, washed once with cold PBS, and lysed in radio immunoprecipitation assay lysis buffer (Beyotime, P0038) containing the protease inhibitor PMSF (Beyotime, ST507). The cell lysate was pre-cleared using 30 μl of protein A/G beads. Equal amounts of total protein lysate were incubated overnight at 4 °C with either anti-USP38 (17767-1-AP, Proteintech), anti-ADAR1 (14330-1-AP, Proteintech) or the normal indicated immunoglobulin G (IgG). Following this, 35 μl of protein A/G beads were added for an additional 2-h incubation. The beads were then washed four times with radio immunoprecipitation assay lysis buffer and heated at 100 °C for 8 min before Western blot analysis.

For mass spectrometry analysis, supernatant was collected from HEK293T cells expressing either Flag-USP38 or an EV (EV-Flag) control. The supernatant was then immunoprecipitated using magnetic beads conjugated to Flag antibody. The proteins enriched by the anti-Flag magnetic beads were digested with trypsin, desalted, and subsequently identified through mass spectrometry (Lumingbio). The raw data were analyzed by Lumingbio Company using ProteomeDiscoverer 2.5 software (ThermoFisher Scientific) and matched against a human protein database. Proteins identified with unique peptides in the Flag-USP38 sample that were more than twice as abundant as those in the EV-Flag control were considered potential USP38 interactors.

For ubiquitination analysis, His-Ub and overexpression plasmids or control plasmids were cotransfected into HEK293T cells. Cells were collected 48 h posttransfection, treated with MG132 (20μM) for 6 h before collection, followed by cell lysis and centrifugation at 17,000×*g* for 30 min, and then subjected to IP with magnetic beads and Western blot analyses.

Immuno-fluorescence staining analyses

For immunofluorescence staining, cells grown on coverslips were first treated with 4% paraformaldehyde fixative, followed by permeabilization with 0.1% Triton X-100. Next, nonspecific binding sites were blocked with 4% bovine serum albumin. Primary antibodies targeting Flag (dilution 1:800, 14793S, Cell Signaling Technology), HA (dilution 1:800, 3724T, Cell Signaling Technology), ADAR (dilution 1:100, sc-271854, Santa Cruz Biotechnology), and USP38 (dilution 1:100, 17767-1-AP, Proteintech) were applied and incubated at 4 °C for 16 h. Subsequent steps were conducted under low-light conditions. Secondary antibodies (CoraLite488-conjugated goat anti-mouse IgG (H + L), SA00013-1; CoraLite594-conjugated goat anti-rabbit IgG (H + L), SA00013-4, proteintech), at a dilution ratio of 1:200, were applied, followed by 4′,6-diamidino-2-phenylindole staining (Beyotime, C1005). Finally, after treating with antifade reagent and sealing the slides, proceed to take photos and visualization using an Olympus confocal laser scanning microscope.

qPCR analyses

For qPCR analysis, total RNA was isolated using the Trizol extraction method and reverse-transcribed with the HiScript III RT SuperMix for qPCR kit (Vazyme, R323). Subsequently, qPCR was conducted using the ChamQ Universal SYBR qPCR Master Mix kit (Vazyme, Q711). qPCR analyses were performed using a CFX Connect Real-Time System (Bio-Rad). qPCR values were calculated using the ΔΔCt method. The primers used for qPCR analysis are detailed in Table S1.

Cellular fractionation

The Nuclear Protein and Cytoplasmic Protein Extraction Kit (Beyotime, P0027) was used for cellular protein extraction as per the manufacturer's instructions. After collecting the cellular precipitate, cytosolic proteins were lysed using reagent A, followed by the addition of 10 μl of cytosolic protein extraction reagent B. The mixture was then centrifuged to retrieve cytoplasmic proteins from the supernatant. The remaining cellular precipitate was lysed with 50 μl of nuclear protein extraction reagent for 30 min at 4 °C, with vigorous shaking every 2 min for 30 s. Postcentrifugation, nuclear proteins were collected from the supernatant. The isolated cytoplasmic and nuclear proteins were then quantified and heat-denatured for Western blot analyses.

CCK-8 assay and colony formation assay

For the CCK-8 assay, 1.5 × 10^3 cells/well (Eca-109 or KYSE-150) were seeded into 96-well plates and incubated overnight. Subsequently, 10 μl of CCK-8 solution (Dojindo, CK04-500T) was added to each well, followed by a 1-h incubation at 37 °C. Absorbance at a wavelength of 450 nm was subsequently quantified utilizing a multimode reader (Molecular Devices, SpectraMax M2). For colony formation assay, cells at a density of 300 per well were seeded into 12-well plates, with the medium being refreshed every 3 days. After 10 to 14 days of culture, colonies were fixed with a 4% fixative

solution and stained with 0.1% crystal violet for 40 min. The colonies were then counted for statistical analysis.

Cell-derived xenograft mouse model

Five-week-old female BALB/c nude mice (Beijing HFK Bioscience Co., Ltd, China) were randomly divided into three groups, with six mice per group. Cells (1 × 10^6) were subcutaneously inoculated into the right neck-back side of each nude mouse (five mice per group). The mice were monitored daily. Tumor sizes were measured using calipers, and tumor volumes were calculated using the formula length × width^2 × 1/2. At predetermined times, the mice were sacrificed, and the tumors were weighed and photographed. All care and experimental procedures involving animals in this study were performed in accordance with the institutional ethical guidelines and were approved by the Ethics Committee of North Sichuan Medical College.

Statistical analysis

Data from three independent *in vitro* experiments were presented as mean ± SD, while data from *in vivo* animal experiments were presented as mean ± SEM. Two-tailed unpaired Student's *t* test was used to compare data between two groups. One/two-way ANOVA with Tukey's test or Bonferroni's test was used for the comparison of multiple groups. p value ≤ 0.05 was considered statistically significant.

Data availability

All data have been provided in this manuscript. All mass spectrometry raw data have been deposited to the ProteomeXchange Consortium (https://proteomecentral.proteomexchange.org) *via* the iProX partner repository with the dataset identifier PXD055320 and are publicly available. Additional details regarding data and protocols supporting the findings of this study are available from the corresponding author upon request.

Supporting information—This article contains supporting information.

Acknowledgments—The authors are grateful to Y. Y. (College of Life Sciences, Sichuan University, Chengdu, China) for providing the plasmid His-Ub used for protein expression. The authors acknowledge the research platform (Innovation Platform) provided by the School of Basic Medical Sciences and Forensic Medicine, North Sichuan Medical College.

Author contributions—Q. H., Y. C., Q. Z., S. D., W. H., Y. Y., C. L., and J. T. writing–review and editing; Q. H. and J. T. writing–original draft; Q. H. and J. T. funding acquisition; Q. H. and J. T. conceptualization; Y. Y. and C. L. resources; Y. C., Q. Z., S. D., W. H., Y. Y., and C. L. data curation; Y. C. visualization; Y. C. validation; Y. C., Q. Z., and S. D. investigation; Q. H. and J. T. methodology.

Funding and additional information—This work was supported by the Municipal and School Science and Technology Strategic Cooperation Project of Nan Chong (grant no. 22SXZRKX0002 and 20SXCXTD004), the Key Cultivation Project of North Sichuan Medical College (grant no. CBY22-ZDA05 and CBY22-ZDA02), the Doctoral Startup Fund Project of North Sichuan Medical College (grant no. CBY21-QD14), the Research and Development Program of the Affiliated Hospital of North Sichuan Medical College (grant no. 2023PTZK024 and 2023PTZK015), and Department of Science and Technology of Sichuan Province (#2022NSFSC0771).

Conflict of interest—The authors declare that they have no conflicts of interest with the contents of this article.

Abbreviations—The abbreviations used are: β-ME, β-mercaptoethanol; ADAR, adenosine deaminase acting on RNA; CCK-8, Cell Counting Kit-8; DUB, deubiquitinating enzyme; ESCC, esophageal squamous cell carcinoma; EV, empty vector; IFN, interferon; IgG, immunoglobulin G; IP, immunoprecipitation; His-Ub, His-tagged ubiquitin; OTU, ovarian tumor protease; qPCR, quantitative PCR; UCH, carboxyl-terminal hydrolase; USP, ubiquitin-specific protease.

References

1. Han, B., Zheng, R., Zeng, H., Wang, S., Sun, K., Chen, R., *et al.* (2024) Cancer incidence and mortality in China, 2022. *J. Natl. Cancer Cent.* **10**, 27–34
2. Abnet, C. C., Arnold, M., and Wei, W. Q. (2018) Epidemiology of esophageal squamous cell carcinoma. *Gastroenterology* **154**, 360–373
3. Song, Y., Li, L., Ou, Y., Gao, Z., Li, E., Li, X., *et al.* (2014) Identification of genomic alterations in oesophageal squamous cell cancer. *Nature* **509**, 91–95
4. Wiwitkeyoonwong, J., Jiarpinitnun, C., Hiranyatheb, P., and Ngamphaiboon, N. (2021) Impact of weight loss on patients with locally advanced esophageal and esophagogastric junction cancers treated with chemoradiotherapy. *Asian Pac. J. Cancer Prev.* **22**, 3847–3855
5. Ajani, J. A., D'Amico, T. A., Bentrem, D. J., Cooke, D., Corvera, C., Das, P., *et al.* (2023) Esophageal and esophagogastric junction cancers, version 2. 2023, NCCN clinical practice guidelines in oncology. *J. Natl. Compr. Canc Netw.* **21**, 393–422
6. Sun, T., Liu, Z., and Yang, Q. (2020) The role of ubiquitination and deubiquitination in cancer metabolism. *Mol. Cancer* **19**, 146–164
7. Liu, J., Cheng, Y., Zheng, M., Yuan, B., Wang, Z., Li, X., *et al.* (2021) Targeting the ubiquitination/deubiquitination process to regulate immune checkpoint pathways. *Signal. Transduct. Target. Ther.* **6**, 28–38
8. Mennerich, D., Kubaichuk, K., and Kietzmann, T. (2019) DUBs, hypoxia, and cancer. *Trends Cancer* **5**, 632–653
9. Kwasna, D., Abdul Rehman, S. A., Natarajan, J., Matthews, S., Madden, R., De Cesare, V., *et al.* (2018) Discovery and characterization of ZUFSP/ZUP1, a distinct deubiquitinase class important for genome stability. *Mol. Cell* **70**, 150–164
10. Li, Y., and Reverter, D. (2021) Molecular mechanisms of DUBs regulation in signaling and disease. *Int. J. Mol. Sci.* **22**
11. Yi, X. M., Li, M., Chen, Y. D., Shu, H. B., and Li, S. (2022) Reciprocal regulation of IL-33 receptor-mediated inflammatory response and pulmonary fibrosis by TRAF6 and USP38. *Proc. Natl. Acad. Sci. U. S. A.* **119**, e2116279119
12. Wang, Y., Li, Q., Hu, D., Gao, D., Wang, W., Wu, K., *et al.* (2021) USP38 inhibits zika virus infection by removing envelope protein ubiquitination. *Viruses* **13**, 2029–2039
13. Zheng, Z., Shang, Y., Xu, R., Yan, X., Wang, X., Cai, J., *et al.* (2022) Ubiquitin specific peptidase 38 promotes the progression of gastric cancer through upregulation of fatty acid synthase. *Am. J. Cancer Res.* **12**, 2686–2696
14. Xu, Z., Hu, H., Fang, D., Wang, J., and Zhao, K. (2021) The deubiquitinase USP38 promotes cell proliferation through stabilizing c-Myc. *Int. J. Biochem. Cell Biol.* **137**, 106023–106030

15. Yang, Y., Yang, C., Li, T., Yu, S., Gan, T., Hu, J., *et al.* (2020) The deubiquitinase USP38 promotes NHEJ repair through regulation of HDAC1 activity and regulates cancer cell response to genotoxic insults. *Cancer Res.* **80**, 719–731
16. Zhan, W., Liao, X., Liu, J., Tian, T., Yu, L., and Li, R. (2020) USP38 regulates the stemness and chemoresistance of human colorectal cancer via regulation of HDAC3. *Oncogenesis* **9**, 48–61
17. Wang, J., Gu, Y., Yan, X., Zhang, J., Wang, J., and Ding, Y. (2023) USP38 inhibits colorectal cancer cell proliferation and migration via down-regulating HMX3 ubiquitylation. *Cell Cycle* **22**, 1169–1181
18. Huang, J., Zhou, W., Hao, C., He, Q., and Tu, X. (2022) The feedback loop of METTL14 and USP38 regulates cell migration, invasion and EMT as well as metastasis in bladder cancer. *PLoS Genet.* **18**, e1010366
19. Chen, S., Yun, F., Yao, Y., Cao, M., Zhang, Y., Wang, J., *et al.* (2018) USP38 critically promotes asthmatic pathogenesis by stabilizing JunB protein. *J. Exp. Med.* **215**, 2850–2867
20. Wang, R., Cai, X., Li, X., Li, J., Liu, X., Wang, J., *et al.* (2024) USP38 promotes deubiquitination of K11-linked polyubiquitination of HIF1alpha at Lys769 to enhance hypoxia signaling. *J. Biol. Chem.* **300**, 105532–105542
21. Lin, M., Zhao, Z., Yang, Z., Meng, Q., Tan, P., Xie, W., *et al.* (2016) USP38 inhibits type I interferon signaling by editing TBK1 ubiquitination through NLRP4 signalosome. *Mol. Cell* **64**, 267–281
22. Patterson, J. B., and Samuel, C. E. (1995) Expression and regulation by interferon of a double-stranded-RNA-specific adenosine deaminase from human cells: evidence for two forms of the deaminase. *Mol. Cell Biol.* **15**, 5376–5388
23. Jiao, Y., Xu, Y., Liu, C., Miao, R., Liu, C., Wang, Y., *et al.* (2024) The role of ADAR1 through and beyond its editing activity in cancer. *Cell Commun. Signal.* **22**, 42–54
24. Herbert, A. (2019) ADAR and immune silencing in cancer. *Trends Cancer* **5**, 272–282
25. Song, B., Shiromoto, Y., Minakuchi, M., and Nishikura, K. (2022) The role of RNA editing enzyme ADAR1 in human disease. *Wiley Interdiscip. Rev. RNA* **13**, e1665
26. Liddicoat, B. J., Piskol, R., Chalk, A. M., Ramaswami, G., Higuchi, M., Hartner, J. C., *et al.* (2015) RNA editing by ADAR1 prevents MDA5 sensing of endogenous dsRNA as nonself. *Science* **349**, 1115–1120
27. Mannion, N. M., Greenwood, S. M., Young, R., Cox, S., Brindle, J., Read, D., *et al.* (2014) The RNA-editing enzyme ADAR1 controls innate immune responses to RNA. *Cell Rep.* **9**, 1482–1494
28. Qin, Y. R., Qiao, J. J., Chan, T. H., Zhu, Y. H., Li, F. F., Liu, H., *et al.* (2014) Adenosine-to-inosine RNA editing mediated by ADARs in esophageal squamous cell carcinoma. *Cancer Res.* **74**, 840–851
29. Anadon, C., Guil, S., Simo-Riudalbas, L., Moutinho, C., Setien, F., Martinez-Cardus, A., *et al.* (2016) Gene amplification-associated overexpression of the RNA editing enzyme ADAR1 enhances human lung tumorigenesis. *Oncogene* **35**, 4407–4413
30. Wei, Y., Zhang, H., Feng, Q., Wang, S., Shao, Y., Wu, J., *et al.* (2022) A novel mechanism for A-to-I RNA-edited AZIN1 in promoting tumor angiogenesis in colorectal cancer. *Cell Death Dis.* **13**, 294–305
31. Li, Y., Wang, N. X., Yin, C., Jiang, S. S., Li, J. C., and Yang, S. Y. (2022) RNA editing enzyme ADAR1 regulates METTL3 in an editing dependent manner to promote breast cancer progression via METTL3/ARHGAP5/YTHDF1 Axis. *Int. J. Mol. Sci.* **23**, 9656–9676
32. Schauer, N. J., Magin, R. S., Liu, X., Doherty, L. M., and Buhrlage, S. J. (2020) Advances in discovering deubiquitinating enzyme (DUB) inhibitors. *J. Med. Chem.* **63**, 2731–2750
33. Wijnhoven, P., Konietzny, R., Blackford, A. N., Travers, J., Kessler, B. M., Nishi, R., *et al.* (2015) USP4 auto-deubiquitylation promotes homologous recombination. *Mol. Cell* **60**, 362–373
34. Zheng, W., Wuyun, Q., Li, Y., Zhang, C., Freddolino, P. L., and Zhang, Y. (2024) Improving deep learning protein monomer and complex structure prediction using DeepMSA2 with huge metagenomics data. *Nat. Methods* **21**, 279–289
35. Haq, S., and Ramakrishna, S. (2017) Deubiquitylation of deubiquitylases. *Open Biol.* **7**
36. Deng, L., Meng, T., Chen, L., Wei, W., and Wang, P. (2020) The role of ubiquitination in tumorigenesis and targeted drug discovery. *Signal. Transduct. Target. Ther.* **5**, 11–38
37. Zhang, T., Su, F., Wang, B., Liu, L., Lu, Y., Su, H., *et al.* (2024) Ubiquitin specific peptidase 38 epigenetically regulates KLF transcription factor 5 to augment malignant progression of lung adenocarcinoma. *Oncogene* **43**, 1190–1202
38. Baker, A. R., and Slack, F. J. (2022) ADAR1 and its implications in cancer development and treatment. *Trends Genet* **38**, 821–830
39. Licht, K., and Jantsch, M. F. (2017) The other face of an editor: ADAR1 functions in editing-independent ways. *Bioessays.* **39**, 1700129–1700134
40. Nemlich, Y., Greenberg, E., Ortenberg, R., Besser, M. J., Barshack, I., Jacob-Hirsch, J., *et al.* (2013) MicroRNA-mediated loss of ADAR1 in metastatic melanoma promotes tumor growth. *J. Clin. Invest.* **123**, 2703–2718
41. Cai, D., Sun, C., Murashita, T., Que, X., and Chen, S. Y. (2023) ADAR1 non-editing function in macrophage activation and abdominal aortic aneurysm. *Circ. Res.* **132**, e78–e93
42. Wolberger, C. (2014) Mechanisms for regulating deubiquitinating enzymes. *Protein Sci.* **23**, 344–353
43. Boudreaux, D. A., Maiti, T. K., Davies, C. W., and Das, C. (2010) Ubiquitin vinyl methyl ester binding orients the misaligned active site of the ubiquitin hydrolase UCHL1 into productive conformation. *Proc. Natl. Acad. Sci. U. S. A.* **107**, 9117–9122
44. Boudreaux, D. A., Chaney, J., Maiti, T. K., and Das, C. (2012) Contribution of active site glutamine to rate enhancement in ubiquitin C-terminal hydrolases. *FEBS J.* **279**, 1106–1118
45. Hu, M., Li, P., Li, M., Li, W., Yao, T., Wu, J. W., *et al.* (2002) Crystal structure of a UBP-family deubiquitinating enzyme in isolation and in complex with ubiquitin aldehyde. *Cell* **111**, 1041–1054
46. Kenny, S., Lai, C. H., Chiang, T. S., Brown, K., Hewitt, C. S., Krabill, A. D., *et al.* (2024) Altered protein dynamics and a more reactive catalytic cysteine in a neurodegeneration-associated UCHL1 mutant. *J. Mol. Biol.* **436**, 168438